On the Complementary Photoluminescent and Electroluminescent Images of Poly(phenylenevinylene)-Based Light-Emitting Diodes with a Thin Active Layer

by **Ivan G. Scheblykin**[a]), **Vladimir I. Arkhipov**[b])[1]), **Mark Van der Auweraer***[a])[2]), and **Frans De Schryver**

[a]) Laboratory for Molecular Dynamics and Spectroscopy, K.U. Leuven, Celestijnenlaan 200 F, B-Leuven 3001
[b]) IPNMC, Philipps-Universität Marburg, Hans-Meerwein-Strasse, D-35032 Marburg

Dedicated to Professor *André M. Braun* on the occasion of his 60th birthday

A clear complementary relationship between photoluminescent (PL) and electroluminescent (EL) images was observed for organic light-emitting diodes (OLEDs) based on poly(phenylenevinylene) (PPV) and dye-doped PPV. So-called 'black spots' (dark circular regions observed on the active area of running OLEDs) become bright ones, when the photoluminescence of the same area is excited. A very small thickness of the active layer (*ca.* 10 nm) was the crucial point to observe this anticorrelation between EL and PL. A substantial increase of the PL yield ('anti-burning' effect) was observed after strong light exposure (*ca.* 10 mJ/cm^2) of the polymer covered by an aluminium layer. The same light exposure without aluminium protection resulted in complete photobleaching of the polymer. The presence of a thin insulating layer between the polymer and aluminium was proposed to be responsible for these effects. This layer prevents electron injection and PL quenching due to exciton dissociation at the metal-polymer interface. The former effect leads to black spots in the EL image, the latter one gives rise to bright spots on the PL image situated on the same places. The intermediate layer can be also induced by light exposure. A very efficient energy transfer from the polymer to the dye and to the J-aggregates of the dye was demonstrated in PPV/dye composite films.

1. Introduction. – Since the discovery of organic electroluminescence more than 10 years ago, great progress has been made in developing organic light-emitting diodes (OLEDs) based on low-molecular-weight molecules or conjugated polymers [1][2]. However, the main obstacle for a wide industrial application of OLEDs is still the quite fast degradation of the devices especially upon running at ambient conditions [1–3].

The formation of the so-called 'black spots' on the active area of an operating OLED is a well-known phenomenon [1][2]. 'Black spots' (BS) are usually circular areas with a very low electroluminiscent (EL) efficiency as compared to the surrounding. The presence of BS leads to long-time degradation of OLEDs made of low-molecular-weight organic molecules [4–6] and polymers [7][8].

Several different mechanisms have been suggested to explain BS formation and growth. The majority of the mechanisms relates to processes occurring at the electrode/organic layer interface: chemical and electrochemical modification of the cathode and/or adjacent organic layer (oxidation, water electrolysis *etc.*), delamination of the electrode [4][5], and interdiffusion of thin layers [9]. It was also shown that degradation of the organic layer itself cannot be a reason for BS formation [5].

[1]) Present address: IMEC, Kapeldreef 75, B-3001 Heverlee-Leuven.
[2]) E-mail: mark.vanderauweraer@chem.kuleuven.ac.be.

Growing BS size during the OLED operation is commonly attributed to a continuous oxygen penetration into the film through initial defects (*e.g.*, pin holes) of the cathode (see, *e.g.* [8]). However, despite great efforts, the situation is still far from clear.

In the present contribution, we report on some interesting observations performed on poly(paraphenylenevinylene)(PPV)-based OLEDs. At variance with the most part of earlier studies, we used OLEDs with a very thin active layer. This small thickness of *ca.* 10 nm (instead of 100 nm in common OLEDs) allowed us to demonstrate very clear relationships between electroluminescent (EL) and photoluminescent (PL) properties of OLED areas subjected to BS degradation.

In our experiments, we used OLEDs made of PPV and of PPV doped with the thiacarbocyanine dye THIATS (*Fig. 1,a*) and its J-aggregates. This dye is well-known to form different kinds of J-aggregates in solution [10][11] as well as in LB [12] and self-assembled [13][14] films. The choice of THIATS allowed us to prepare a stable solution of J-aggregates and pre-PPV in H_2O, while it was not possible for the dye 5,5′,6,6′-tetrachloro-1,1′-diethyl-3,3′-bis(4-sulfobutyl)benzimidazolocarbocyanine (TDBC) [15] [16] due to incompatibility of the pH of the mixed compounds. Being dispersed in an electroactive polymer, aggregated dye species act as extended traps for charge carriers and very effective fluorescent recombination centers [15–17]. These properties make J-aggregates and dye nanocrystals quite interesting systems for electroluminescence applications.

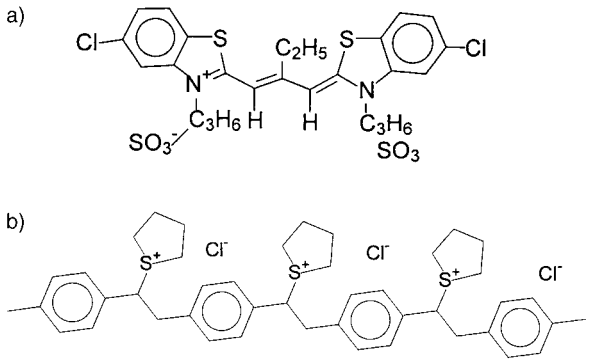

Fig. 1. *Chemical structure of* a) *the cyanine dye THIATS*, and b) *the tetrahydrothiophenium PPV-precursor (pre-PPV)*

Experimental. – The positively charged H_2O-soluble PPV precursor (pre-PPV, *Fig. 1,b*) was synthesized starting from *p*-xylylenebis[tetrahydrothiophene] chloride (*Aldrich*). The synthesis and purification were carried out as described in [18][19]. The 5,5′-dichloro-9-ethyl-3,3′-bis[3-sulfopropyl]thiacarbocyanine (THIATS, *Fig. 1,a*) was supplied by *AGFA*.

Mixing an aq. soln. of the negatively charged THIATS dye with an aq. soln. of the positively charged pre-PPV was found to cause extensive aggregation. Upon mixing, the maximum of the absorption spectrum shifted from 550 nm, corresponding to dye monomers in H_2O, to 625 nm, which is absorption band typical of J-aggregates [10], while the width of the band was reduced to 10–15 nm (250–400 cm^{-1}). In this solution, J-aggregates revealed a high fluorescence quantum yield of *ca.* 40%, and a narrow fluorescence band at around 630 nm.

Two types of aq. solns. were prepared: *i*) pure pre-PPV soln. with the concentration of monomer of $2 \cdot 10^{-2}$ M and *ii*) PPV/THIATS composite solns. with the concentrations of pre-PPV starting from $2 \cdot 10^{-2}$ M

(monomer concentration) and the concentration of THIATS *ca.* 10^{-3} M. The films were prepared by spin coating at a rotation speed of 1500 rpm at r.t. In the composite films, the final ratio of PPV and THIATS (molar concentrations of monomers) varied from 40:1 to 1000:1 in different samples.

The films were deposited on either ITO glass (purchased from *Merck*) or ordinary cover glass. The substrates were cleaned in sonicated 1% KOH in H_2O/EtOH 3:7 soln. at 50° during 20 min and afterwards in H_2O. In some samples (see below), we used an additional layer of poly(*N*-vinylcarbazole) (PVK) between ITO and the emissive layer. PVK of the molecular weight 1,100,000 was provided by *Aldrich*. The PVK layer was spin-coated from 4 mg/1 ml soln. of PVK in 1,2-dichlorobenzene at 1500 rpm at r.t.

Thermal conversion of pre-PPV into the conjugated polymer was carried out by heating the samples in 10^{-3} Torr vacuum at 150° during 11 h. Due to a low concentration of pre-PPV in the aq. soln. and a slow water evaporation during the spin coating at r.t., the thickness of prepared films was as small as 10–15 nm after the conversion of the precursor into PPV. The film thickness was estimated from topographic profiles of 'scratched' samples measured on an atomic-force microscope (*Topometrics Explorer*). It is worth noting that this value of the thickness is at least 5–10 times less than the thickness of PPV layers typically used in PPV-based OLEDs [1].

In a later stage the reproducibility of the results was checked using a commercially available aq. soln. of the same PPV precursor from *LARK Enterprises*, USA.

OLEDs of the following types were fabricated: Type 1: ITO/PVK (20 nm)/PPV (15 nm)/Al; Type 1A: ITO/PPV (15 nm)/Al; Type 2: ITO/PVK (20 nm)/PPV + THIATS (10–15 nm)/PPV (15 nm)/Al.

The PVK layer was used to reduce the hole injection from ITO ($HOMO_{PVK} \approx 6$ eV, *Work Function* $_{ITO} \approx 5$ eV) resulting in a more balanced injection of electrons and holes into the device, and an enhanced electroluminescence yield. Aluminium layers were evaporated in 10^{-4} Torr vacuum on the top of the films. The devices were stored in the dark under ambient conditions and run under ambient conditions without any further precautions. Photoluminescence spectra of the samples were measured by spectrofluorimeter *Fluorolog 1691, SPEX*.

A sketch of the experimental setup for measurements of PL and EL images is shown in *Fig. 2*. Photoimages of OLEDs excited by 400-nm light (PL image, *Fig. 2,a*) and by electrical current (EL image, *Fig. 2,b*) were obtained by the use of an optical microscope *OPTIPHOT-2* (*Nikon*) with episcopic fluorescence attachment *Nikon EFD-3* coupled to a photo-camera *Nikon FX-35WA*. The total magnification was 100 times. A typical exposure of an *ISO 800* photographic film was *ca.* 5–20 s to obtain a PL image and *ca.* 300 s to obtain an EL image. Excitation of the PL was carried out by the standard Hg lamp of the episcopic fluorescence attachment. The wavelength region from 380 to 420 nm was selected from the lamp spectrum by a band-pass filter *EX380-420* and a dichroic mirror *DM430* (*Nikon*). Fluorescence was observed through a long-pass filter *BA450* (*Nikon*). To obtain PL images, the total intensity of the lamp was decreased with a neutral density filter by a factor of 16. The same Hg lamp was used for light-induced stressing of the polymer film in photodegradation experiments. No filters were used in that case, and the power of the light measured in the focal plate of the microscope was *ca.* 16 mW/cm^2. The size of the exposed area was adjusted with a diaphragm.

Electroluminescence spectra were collected by *IRRAD2000 Miniature Fiber Optics Spectrometer* (*Ocean Optics, Inc.*) coupled with a PC.

Results and Discussion. – 1. *Photo- and Electroluminescence of the Films.* After the heat treatment, pre-PPV films revealed absorption spectra with a maximum at 430 nm and fluorescence spectra with a first maximum at 510 nm, which was typical of PPV [18][20]. The fluorescence quantum yield of the PPV film deposited on a quartz substrate was *ca.* 10–15%, which is also in agreement with the data known from the literature [21].

The absorption spectrum of the PPV/THIATS composite film after the heat treatment revealed a very weak band at 550–580 nm in addition to the characteristic 400–450-nm PPV band. This weak band corresponds to absorption of the dye monomers and short dye aggregates. The molar extinction coefficient of THIATS in MeOH at 550 nm is 90000, while that of a PPV oligomer with three phenylene vinylene units is *ca.* 70000 at 360 nm [22]. Hence, a very crude estimation indicates that the extinction of a single THIATS molecule matches that of three phenylene vinylene units in PPV. In this case, for the ratio of molar concentrations of THIATS and PPV of 1:100,

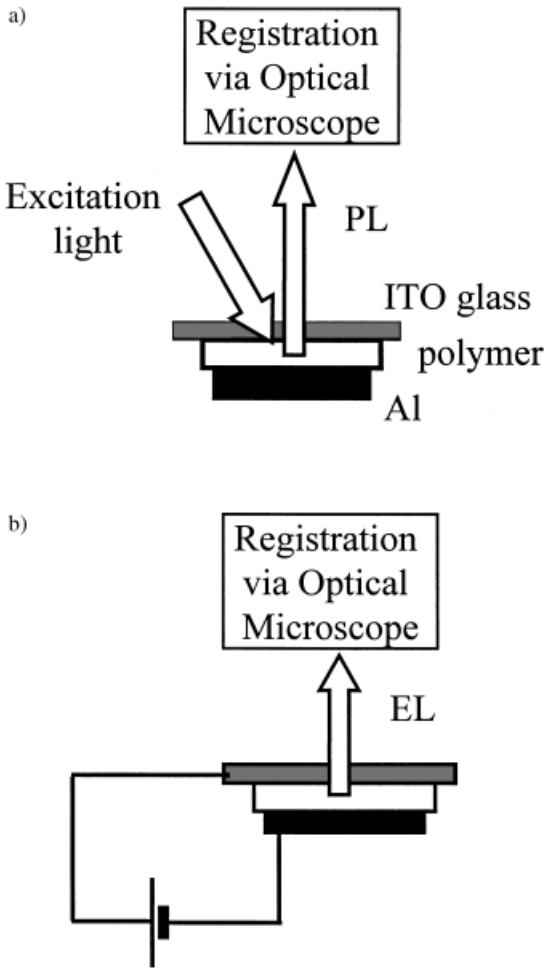

Fig. 2. a) *Imaging of the OLED in photoluminescent light* (PL image), *and* b) *imaging in electroluminescent light* (EL image)

one would expect a ratio of integrals under the absorption bands of PPV and THIATS of *ca.* 1:30 that fits the experimentally observed value.

However, in contrast with the absorption spectrum, a significant portion of the total fluorescence emission originates from the dye. Fluorescence spectra of the PPV/THIATS composite films, excited at 430 nm *via* PPV absorption band, are shown in *Fig. 3*. The spectrum exhibits both PPV-related bands at 510 and 540 nm, and a red band in the range of 600–650 nm. We attribute this long-wavelength fluorescence to aggregated dye species. Comparing the fluorescence spectra of the dye in the composite film before and after pre-PPV conversion indicates that disruption of dye packing in the aggregates must have happened during the heating. Upon heating, the red band of PPV/THIATS composite film fluorescence spectra became as broad as 1300 cm^{-1} and less red-shifted with the maximum at *ca.* 605–610 nm instead of 625 nm before

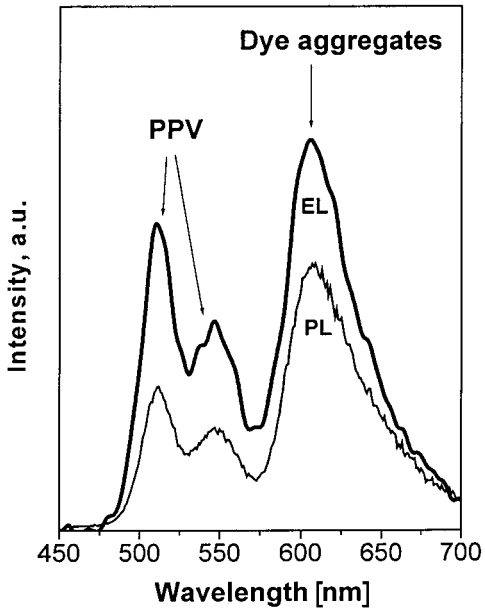

Fig. 3. *Photoluminescence* (thin line) *and electroluminescence spectra of the PPV/THIATS composite LED* (Type 2)

heating. This effect is probably due to drastic changes in the film morphology and the loss of charged groups during the pre-PPV conversion to the conjugated polymer. We suggest that this spectrum is characteristic of short disordered dye aggregates (dimers, trimers, *etc.*) and, possibly, also of nonaggregated monomers in polar surroundings. A detailed study of the excited-state dynamics in PPV/THIATS composite films will be published elsewhere [20][23].

Despite the relatively low concentration of the dye in the composite films, *ca.* 50% of the total fluorescence excited at 430 nm, *i.e.*, at the maximum of the PPV band, originates from the dye (see *Fig. 3*). One should bear in mind that the dye extinction is vanishingly small compared to that of PPV, especially at this wavelength. One can, therefore, conclude that a very efficient energy transfer (ET) occurs from the initially excited polymer to the dye. In this process, dye molecules act as fluorescent traps for excitations localized on PPV chains. The excitation spectrum of the 610 nm band almost coincides with the absorption band of PPV. The fluorescence quantum yield of the PPV/THIATS film, deposited on a glass substrate, was estimated as *ca.* 6–10% when excited *via* the PPV absorption band. This also indicates that a low concentration of the dye dopant in a PPV film does not lead to a drastic decrease of the fluorescence ability of the material.

Several mechanisms may be responsible for the ET from polymer chains to dye molecules. The first one to be mentioned is the conventional *Förster* ET. One could expect this mechanism to be quite important due to the substantial overlap of the PPV fluorescence spectrum and the absorption band of dye aggregates at 580–610 nm. The second mechanism can be exciton diffusion towards dye species followed by exciton

trapping [24]. It is also energetically feasible that geminate pairs of electrons and holes recombine into excitons on dye molecules, leading to light emission after recombination. The study of the temperature dependence of the ET, which is currently in progress, may help to distinguish between those mechanisms [23].

Due to the very small thickness of the polymer layer, the degradation of all types of OLEDs, fabricated as described under *Experimental*, occurred within tens of minutes. A quite bright EL was observed during first several tens of seconds or a few minutes after switching on the current. A typical current density ranged from 10 to 200 mA/cm^2 at the bias voltage from 2 to 8 V for fresh and aged samples, respectively.

We also found that the average brightness can be substantially increased by running the OLED under a 'chopped' current regime with a switch interrupting the current with a frequency of *ca.* 5 Hz. 'Off' and 'On' times were approximately equal to each other. Such an operating regime did extend the OLED active lifetime by several times. This effect is probably caused by charge carrier release from traps while the external voltage was switched off. Carrier detrapping was also suggested as a possible explanation of the so-called 'injectionless EL,' which was recently observed in PPV and MEH-PPV OLEDs [25][26].

2. *Complementary PL and EL Images.* PL and EL images of two type-1 OLEDs are presented in *Figs. 4*,*a* and *b*. The only difference between these two samples is that one of them (*Fig. 4*,*b*) was probed soon after fabrication, while *Fig. 4*,*a*, shows the image of an aged OLED. Hereafter, an OLED, which has been fabricated several weeks prior to the experiment, and whose resource has been already substantially exhausted, will be referred as to an aged OLED. The EL image of the fresh OLED reveals the classical black spot picture (see *Fig. 4*,*b*). For the aged OLED, the dark areas in EL are much larger and have more diverse shapes than the simple circles evidenced by *Fig. 4*,*a*.

Comparing the EL and PL images of the same samples clearly shows that these images are complementary. The bright regions on the PL image were dark in the EL image and *vice versa*. The black spots of the EL image thus become bright spots when the film is excited by light. In the other words, the EL image is a negative of the PL image.

The occurrence of this phenomenon did not depend on the size of dark areas in the EL image, and it was observed on all types of OLEDs studied in the present work including OLEDs type-1A made of the precursor purchased from *Lark Enterprises*, USA. In PPV/THIATS composite type-2 OLEDs, the effect was slightly less prominent probably due to doubling the layer thickness. There are practically no indications of such an effect in the literature. To our knowledge, only *McElvain et al.* [5] recently reported a slight increase of the BS brightness in the PL image of Alq_3-based OLEDs. However, no further attention was paid to and no explanation was suggested for that interesting phenomenon.

To understand the anticorrelation between PL and EL images, the exciton-quenching processes must be considered in a thin polymer layer covered by a metal. Two conventional mechanisms of the exciton quenching by a metal electrode were discussed in the literature. The first one is the irreversible energy transfer from an excited polymer segment to the metal. This well-known mechanism is governed by the long-range dipole-dipole interaction between the exciton and its mirror twin [27][28] as illustrated in *Fig. 5*,*a*. A more sophisticated version of this model also takes into account exciton diffusion from the bulk of the polymer film towards the metal-polymer

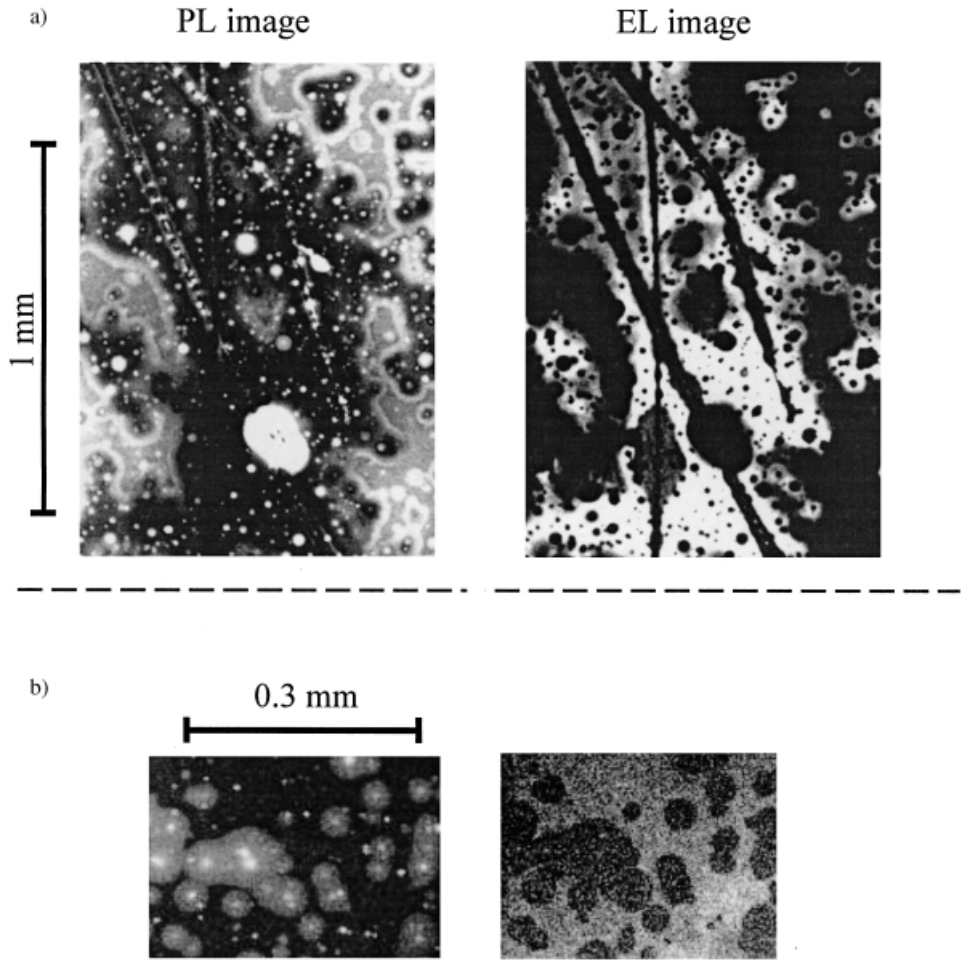

Fig. 4. *PL and EL images of the same area of a PPV-only LED* (Type 1). EL Images were obtained for a bias of 3 V and a current density of 40 mA/cm^2.

interface [29]. Hereafter, this model will be referred as to *long-range quenching model*. One should bear in mind that this quenching mechanism is rather insensitive to the presence of a thin intermediate insulating layer in between a polymer and a metal electrode [29].

The second quenching mechanism is attributed to the dissociation of excitons at the metal-polymer interface [28][30]. This *interfacial quenching mechanism* is sketched in *Fig. 5*, *a*. In the case of direct contact between a polymer and a metal electrode, the rate of the interfacial quenching can be estimated on the basis of the so-called absorbing-wall model, which suggests that an exciton dissociates as soon as it reaches the metal. Note that, contrary to the long-range-quenching mechanism, the rate of the interfacial quenching drastically depends on the presence of an intermediate insulating layer on the metal surface. This mechanism simply does not work if such a layer is present. Both

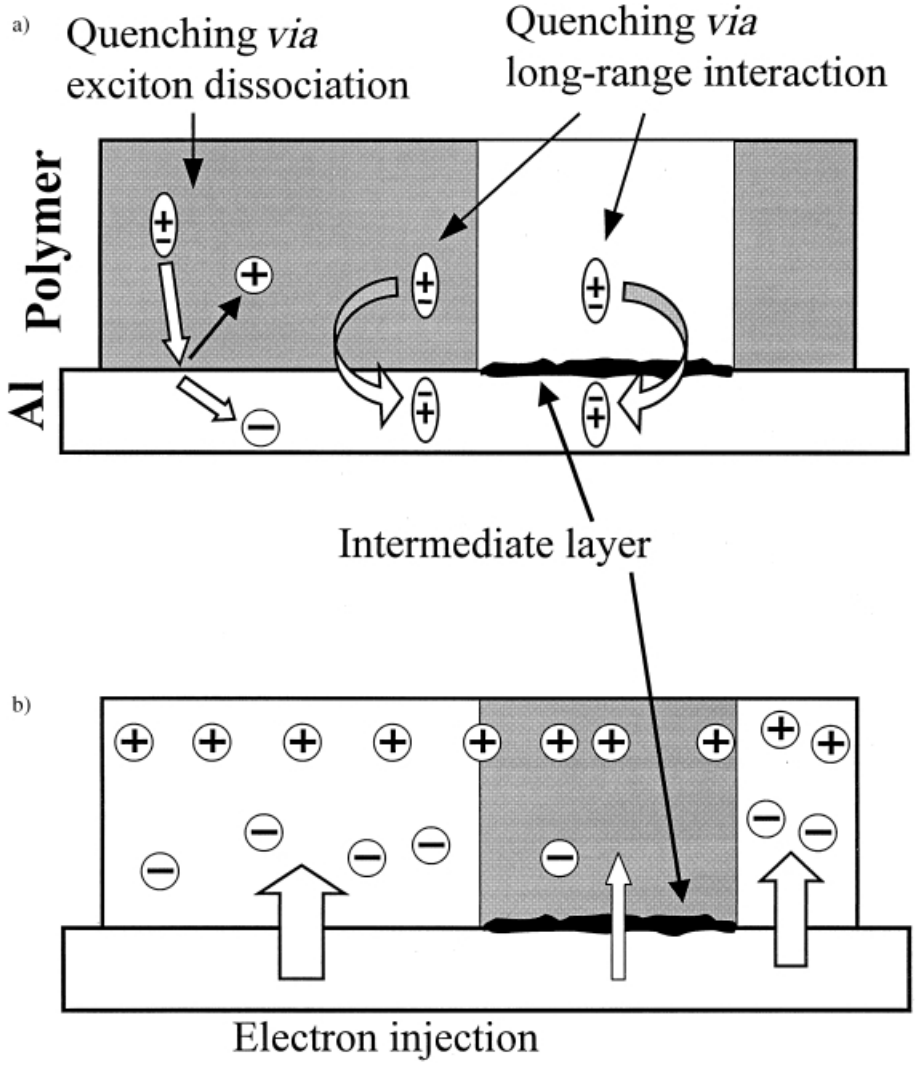

Fig. 5. a) *Two mechanisms of the exciton quenching at a metal-polymer interface* (formation of the bright spots in PL image). b) *Formation of the black spots in EL image.*

quenching processes were considered in [29] as possible causes of the electrode-assisted PL quenching in Alq_3 films [31]. However, the authors admitted that the available experimental data were insufficient to completely preclude one of these mechanisms.

The anticorrelation between PL and EL images can be rationalized in terms of the contact-assisted quenching of singlet excitations. More specifically, we attribute this effect to the formation of an insulating intermediate layer between the polymer and the Al electrode. On the one hand, such modification of the interface leads to a reduction of the electron injection and to a concomitant decrease of the EL intensity as illustrated

in *Fig. 5,b*. On the other hand, it suppresses the *interfacial quenching* of PL and, thus, enhances the PL yield. However, further experiments are needed to understand the origin of such a modification of the interface. It could be either formation of a thin aluminium oxide layer or modification of the interface due to covalent bonds formation between Al and the polymer (see [32] for details). Such an intermediate layer has also been suggested to play an important role in time-dependent EL dynamics after switching on/off the current [26].

If the thickness of a polymer layer is comparable to the exciton diffusion length, which is around 5 nm in PPV [24][33], the PL characteristics of this layer are mainly determined by the processes at the polymer-electrode interface. In contrast to thicker samples, the bulk fluorescence no longer hides the phenomena affecting the fluorescence that originates at the interfacial region. Therefore, the very small 5–15 nm thickness of polymer layers in our samples provides for a dominant contribution of the metal-polymer interface to the observed effects.

3. *Light-Induced Degradation of Polymer Layers and Formation of Artificial Black Spots.* A major drawback of the PPV-based OLEDs is the poor stability of the polymer against oxygen (see, *e.g.*, review papers [1][2]). Furthermore, this degradation is enhanced by light exposure of the unsealed polymer [24]. It is the oxygen-induced degradation that motivated fabrication, storage, and operation of PPV-based OLEDs in vacuum. A metal deposition on top of the film is a well-known remedy of suppressing polymer oxidation and fast photobleaching [34]. Covering a thin fluorescent film with an Al layer is widely used in the single-molecule spectroscopy where the light stress per a single molecule is very high indeed. This method was successfully applied to prevent fast photobleaching of single MEH-PPV chain [34]. Furthermore, nearly all OLEDs are covered with metal electrodes that provide some protection against oxidation even under atmospheric exposure of the device.

To reveal the extent of such a protection a PPV/THIATS film on a glass substrate, partially covered by Al, was exposed to an intense light source. The results are shown in *Fig. 6*. While the PL of the unsealed polymer bleached within a few minutes under the 400 nm illumination with an intensity of 16 mW/cm^2, nearly no bleaching occurred under the same conditions within the area covered by Al. In contrast to the generally expected light-induced PL degradation, quite a substantial increase of the PL yield was observed in some films upon light exposure. This *antiburning* effect was also observed in thin PPV films regardless of the presence of either ITO or PVK layers. The effect was also confirmed for PPV films made of the commercially available (*Lark*, USA) water-soluble PPV precursor. Similarly to the complementary relationship between PL and EL images, the *antiburning* effect can be explained by the light-assisted formation of an intermediate insulating layer in between the polymer and Al contact, which blocks the interfacial quenching and increases the PL yield.

The *antiburning* effect was also observed in some OLEDs in which ITO and/or PVK layers were present below the PPV layer. However, the effect was normally less pronounced and depended somehow on the current stress the OLED had suffered before. The EL from light-exposed areas was always less intense than before exposure, even for those sites that became brighter in PL due to the *antiburning* effect. This proves that light can create, in some samples, areas revealing the same complementary behavior of PL and EL images as in 'black spots areas' observed in fresh and degraded OLEDs.

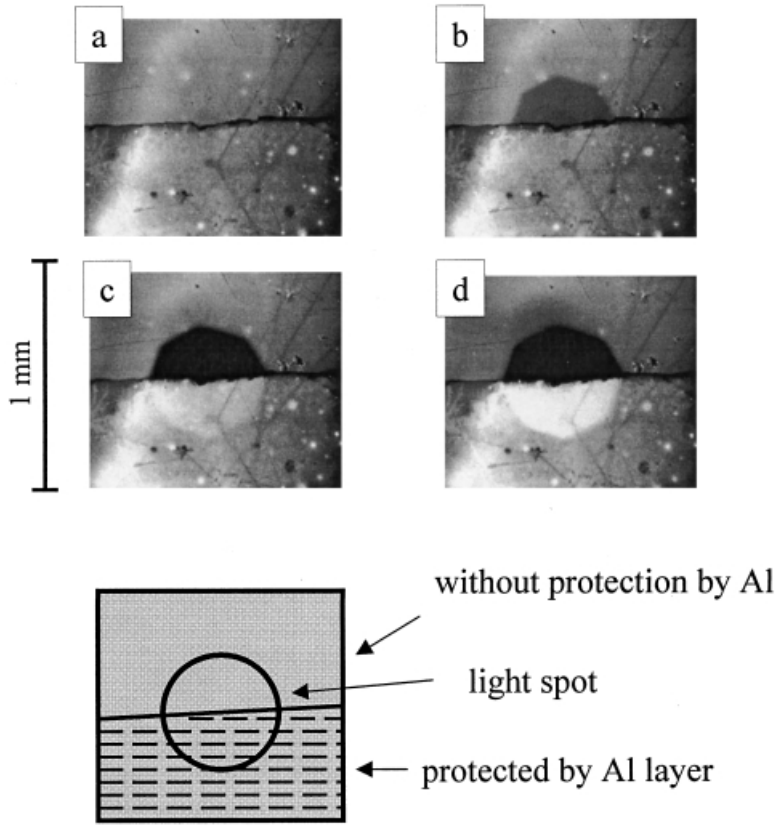

Fig. 6. *PPV/THIATS Composite-film degradation under intensive light exposure.* The film was deposited on the glass substrate and partially covered by Al layer. PL Images were taken *via* a fluorescence microscope (see the text for details). *a*) fresh sample; *b*) exposure = 0.3 J cm$^{-2;}$ *c*) exposure = 5 J cm^{-2}; *d*) exposure = 25 J cm^{-2}.

The effect of fast photobleaching of unsealed PPV may be used for testing OLEDs for presence of areas into which oxygen and/or water has penetrated. Black spots are commonly suggested to be such places. To verify this idea, aged OLEDs with a large density of black spots were stressed by the light exposure in excess of 25 J/cm^2. However, absolutely no decrease of the PL within and around those BS was found. It is worth noting that this exposure caused complete degradation of the polymer without Al coverage. This observation apparently contradicts the idea that the continuous penetration and diffusion of oxygen (or water) is indeed the main reason of the BS growth in OLEDs.

Conclusions. – *1*) A clear complementary relationship between PL and EL images was observed in thin PPV-based OLEDs. Black spots on the OLED active area, observed during the operation, become bright ones when the photoluminescence of the same area was excited.

2) The increase of the photoluminescence yield was observed after strong light exposure of the polymer covered by an Al layer.

3) The same anticorrelation between PL and EL images was observed in OLEDs exposed to an intense light. Exposed areas were dark in EL and bright in PL.

All these phenomena can be explained by formation of a thin insulating layer between the polymer and the Al contact. This layer not only reduces the electron injection, as has been extensively discussed in the literature, but also suppresses exciton dissociation at the metal-polymer interface. The former effect leads to the occurrence of black spots in the EL image, while the latter yields bright spots on the PL image situated at equivalent places. How this intermediate layer can also be induced by light exposure is a subject for further investigation. Our observations indicate an important role for fluorescence quenching due to exciton dissociation at the metal-polymer interface.

This work was supported by *NATO* grant SfP97-1940. *I. G. Sch.* thanks the *F. W. O.* (*Fonds voor Wetenschappelijk Onderzoek Vlaanderen*) for a 'Visiting Postdoctoral Fellowship' and the *K. U. Leuven* for a 'Junior Research Fellowship'. *V. I. A.* is grateful to the *Stiftung Volkswagenwerk* for the financial support. The authors gratefully acknowledge the continuing support from *DWTC* (Belgium) through grant IUAP-IV-11, the *F. W. O.-Vlaanderen*, the *K. U. Leuven Research Fund* through GOA 2001/2, the *European Union* through Cost D14, and the *Nationale Loterij*. The authors thank Dr. *Hua Zhang* for help with AFM measurements. The authors are grateful for *Agfa N. V.* for the sample of THIATS.

REFERENCES

[1] R. H. Friend, R. W. Gymer, A. B. Holmes, J. H. Burroughes, R. N. Marks, C. Taliani, D. D. C. Bradley, D. A. Dos Santos, J. L. Bredas, M. Lögdlund, W. R. Salaneck, *Nature* **1999**, *397*, 121.
[2] L. J. Rothberg, A. J. Lovinger, *J. Mater. Res.* **1996**, *11*, 3174.
[3] H. Azis, G. Xu, *Synth. Met.* **1996**, *80*, 7.
[4] Y.-F. Liew, H. Azis, N.-X. Hu, H. S.-O. Chan, G. Xu, Z. Popovic, *Appl. Phys. Lett.* **2000**, *77*, 2650.
[5] J. McElvain, H. Antoniadis, M. R. Hueschen, J. N. Miller, D. M. Roitman, J. R. Sheats, R. L. Moon, *J. Appl. Phys.* **1996**, *80*, 6002.
[6] L. M. Do, E. M. Han, Y. Niidome, M. Fujihira, T. Kanno, S. Yoshida, M. Maeda, A. J. Ikushima, *J. Appl. Phys.* **1994**, *76*, 5118.
[7] B. H. Cumpston, K. F. Jensen, *Appl. Phys. Lett.* **1996**, *69*, 3941.
[8] S. H. Kim, H. Y. Chu, T. Zyung, L.-M. Do, D.-H. Hwang, *Synth. Met.* **2000**, *111 – 112,* 253.
[9] M. Fujihira, L. M. Do, A. Koike, E.-M. Han, *Appl. Phys. Lett.* **1996**, *68*, 1787.
[10] M. A. Drobizhev, M. N. Sapozhnikov, I. G. Scheblykin, M. Van der Auweraer, O. P. Varnavsky, A. G. Vitukhnovsky, *Chem. Phys.* **1996**, *211*, 455.
[11] I. G. Scheblykin, O. Yu. Sliusarenko, L. S. Lepnev, A. G. Vitukhnovsky, M. Van der Auweraer, *J. Phys. Chem. B* **2001**, *105*, 4636.
[12] N. Vranken, M. Van der Auweraer, F. De Schryver, H. Lavoie, P. Bélanger, C. Salesse, *Langmuir* **2000**, *16*, 9518.
[13] N. Kometani, H. Nakajima, K. Asami, Y. Yonezawa, O. Lajimoto, *J. Phys. Chem. B* **2000**, *104*, 9630.
[14] E. Rousseau, M. Van der Auweraer, F. C. De Schryver, *Langmuir* **2000**, *16*, 8865.
[15] S. Bourbon, M. Gao, S. Kirstein, *Synth. Met.* **1999**, *101*, 153.
[16] S. Kirstein, S. Bourbon, M. Y. Gao, U. De Rossi, *Isr. J. Chem.* **2000**, *40*, 129.
[17] E. I. Mat'tsev, D. Lypenko, B. I. Shapiro, M. A. Brusentseva, G. H. W. Milburn, J. Wright, A. Hendriksen, V. I. Berendyaev, B. V. Kotov, A. V. Vannikov, *Appl. Phys. Lett.* **1999**, 75, 1896.
[18] D. R. Gagnon, J. D. Capistran, F. E. Karasz, R. W. Lenz, S. Antoun, *Polymer* **1987**, *28*, 567.
[19] J. M. Machado, F. E. Karasz, R. F. Kovar, J. M. Burnett, M. A. Druy, *New Polymeric Mater.* **1989**, *1*, 189.
[20] I. G. Scheblykin *et al.*, in preparation.
[21] N. C. Greenham, I. D. W. Samuel, G. R. Hayes, R. T. Phillips, Y. A. R. R. Kessener, S. C. Moratti, A. B. Holmes, R. H. Friend, *Chem. Phys. Lett.* **1995,** *241*, 89.

[22] I. B. Berlman, ' Handbook of fluorescence spectra of aromatic molecules', 2nd ed., Academic Press, New York and London, 1971, p. 324.
[23] I. G. Scheblykin, L. S. Lepnev, A. G. Vitukhnovsky, M. Van de Auweraer, *J. Lumin.* **2001**, in press.
[24] M. Yan, L. J. Rothberg, F. Papadimitrakopoulos, M. E. Galvin, T. M. Miller, *Phys. Rev. Lett.* **1994**, *73*, 744.
[25] A. V. Yakimov, V. N. Savvate'ev, D. Davidov, *Synth. Met.* **2000**, *115*, 51.
[26] J. M. Lupton, V. R. Nikitenko, I. D. W. Samuel, H. Bässler, *J. Appl. Phys.* **2001**, *89*, 311.
[27] R. R. Chance, A. Prock, R. Silbey, *J. Chem. Phys.* **1975**, *62*, 2245.
[28] M. Pope, C. E. Swenberg, 'Electronic Processes in Organic Crystals and Polymers', Oxford University Press, 1999, Chapt. 2E, pp. 326–330.
[29] A. L. Burin, M. Ratner, *J. Phys. Chem. A* **2000**, *104*, 4704.
[30] S. Barth, H. Bässler, H. Rost, H. H. Hörhold, *Phys. Rev. B* **1997**, 56, 3844.
[31] V. E. Choong, Y. Park, Y. Gao, *J. Vac. Sci. Technol. A* **1998**, *16*, 1838.
[32] W. S. Salaneck, J. L. Bredas, *Adv. Mater.* **1996**, *8*, 48.
[33] M. Pope, C. E. Swenberg, 'Electronic Processes in Organic Crystals and Polymers', Oxford University Press, 1999, Chapt. 9, pp. 825–854.
[34] J. Yu, D. Hu, P. F. Barbara, *Science* **2000**, *289*, 1327.

Received May 25, 2001